

Amplified Rate Acceleration by Simultaneous Up-Regulation of Multiple Active Sites in an Endo-Functionalized Porous Capsule

Sivil Kopilevich,[†] Achim Müller,[‡] and Ira A. Weinstock^{*,†}

[†]Department of Chemistry, Ben Gurion University of the Negev, Beer Sheva 84105, Israel

[‡]Faculty of Chemistry, University of Bielefeld, Bielefeld D-33501, Germany

S Supporting Information

ABSTRACT: Using the hydrolysis of epoxides in water as a model reaction, the effect of multiple active sites on Michaelis–Menten compliant rate accelerations in a porous capsule is demonstrated. The capsule is a water-soluble I_h -symmetry Keplerate-type complex of the form, $[\{\text{Mo}^{\text{VI}}\text{O}_{21}(\text{H}_2\text{O})_6\}_{12}\{\text{Mo}^{\text{V}}_2\text{O}_4(\text{L})\}_{30}]^{42-}$, in which 12 pentagonal “ligands,” $\{(\text{Mo}^{\text{VI}})\text{Mo}^{\text{VI}}_5\text{O}_{21}(\text{H}_2\text{O})_6\}^{6-}$, are coordinated to 30 dimolybdenum sites, $\{\text{Mo}^{\text{V}}_2\text{O}_4\}^{1+}$ (L = an endohedrally coordinated η^2 -bound carboxylate anion), resulting in 20 Mo_9O_9 pores. When “up-regulated” by removal of ca. one-third of the blocking ligands, L, an equal number of dimolybdenum sites are activated, and the newly freed-up space allows for encapsulation of nearly twice as many substrate guests, leading to a larger effective molarity (amplification), and an increase in the rate acceleration ($k_{\text{cat}}/k_{\text{uncat}}$) from 16,000 to an enzyme-like value of 182,800.

With the aim of modeling the behaviors of natural enzymes, supramolecular chemistry has been used to design sophisticated structures for catalytic transformations of substrates.¹ Along with recognition or encapsulation, size- and enantioselectivity,² regulation and even reversible allosteric control^{1g,3} have been realized. In several cases, very large rate accelerations^{1b,4} have been achieved via combinations of proximity effects, the influences of specific physicochemical properties of host complexes, and the inclusion of catalytic active sites.

For metal–ligand cages and containers, however, the incorporation of catalytically active metal centers remains an ongoing challenge.^{1a–c,e,f} One reason is that main-group and transition metal cations present as structural components are usually coordinatively saturated or sterically inaccessible to encapsulated substrates. In response, organometallic complexes themselves are being incorporated as reactive guests,^{1b,c,2d,5} and more flexible and tunable metal–ligand structures are being developed in which the relative positions of active metal centers are controlled by chemical switches.^{1g,3} Nevertheless, nanocontainers in which structurally integral metal centers serve as catalytic sites for encapsulated substrates are relatively rare.⁶

One intriguing example, however, is provided by water-soluble I_h -symmetry “Keplerate”-type capsules of the general form $[\{\text{Mo}^{\text{VI}}_6\text{O}_{21}(\text{H}_2\text{O})_6\}_{12}\{\text{Mo}^{\text{V}}_2\text{O}_4(\text{L})\}_{30}]^{42-}$ $\{\text{Mo}_{132}\}$ (Figure 1A).⁷ Here, 30 bimetallic sites, $\{\text{Mo}^{\text{V}}_2\text{O}_4\}^{1+}$ ($\text{Mo}^{\text{V}}_2\text{L}$, where L is an endohedrally⁸ coordinated η^2 -bound carboxylate

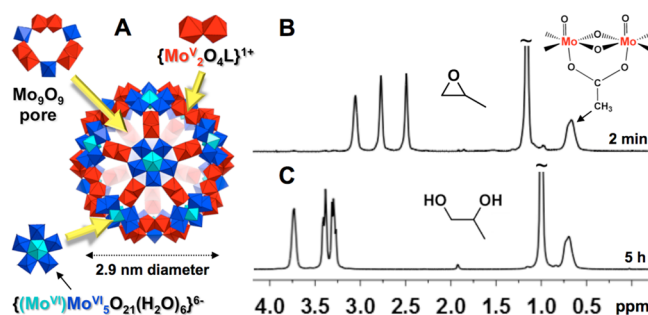


Figure 1. Hydrolysis of propylene oxide (PO, 70 equiv) by a $\{\text{Mo}_{132}\}$ -type capsule (A, in polyhedral notation) at room temperature (296 ± 1 K) in D_2O . (B,C) ^1H NMR spectra before and after hydrolysis of PO. Inset to B: an η^2 -bound acetate ligand, L, coordinated to a Mo^{V}_2 active site; the broad signal at 0.7 ppm arises from the Me groups of the capsule’s 23 internal acetate ligands, L.

anion; inset to panel B),⁹ are coordinated by negatively charged pentagonal “ligands,” $\{(\text{Mo}^{\text{VI}})\text{Mo}^{\text{VI}}_5\text{O}_{21}(\text{H}_2\text{O})_6\}^{6-}$, resulting in 20 Mo_9O_9 rings that serve as size-selective pores.¹⁰ When L in $\text{Mo}^{\text{V}}_2\text{L}$ is replaced by labile water molecules, the resultant $\text{Mo}^{\text{V}}_2(\text{H}_2\text{O})_2$ units (abbreviated Mo^{V}_2) function as combined Lewis-acid and proton-relay sites.¹¹

Using the hydrolysis of epoxides as a model reaction (Figure 1), we now show how Keplerate-type capsules can be tuned to display Michaelis–Menten kinetics, after which, “up-regulation” by removal of 11 endohedrally coordinated acetate ligands, L, from the capsule’s $\text{Mo}^{\text{V}}_2\text{L}$ units lead to a more than 10-fold increase in rate acceleration, $k_{\text{cat}}/k_{\text{uncat}}$, to an enzyme-like value of 182,000. We further show that the kinetic effect of the larger number of Mo^{V}_2 sites is amplified by an increase in effective molarity arising from occupancy of the (now) less congested capsule by a larger number of epoxide guests.

The ^1H NMR spectra in Figure 1B,C show propylene oxide (PO), before and after its hydrolysis to 1,2-propanediol by a $\{\text{Mo}_{132}\}$ -type capsule (3.61 mM) containing 23 acetate-ligand-blocked linkages, $\text{Mo}^{\text{V}}_2\text{L}$, and seven activated (acetate-free) Mo^{V}_2 units with labile water ligands, i.e., $\text{Mo}^{\text{V}}_2(\text{H}_2\text{O})_2$. A kinetic plot obtained by integration of ^1H NMR signal intensities (Figure S1) showed 100% conversion within ca. 6 h. In the absence of the capsule, less than 0.5% of the epoxide was converted to products over the same time period.

Received: June 15, 2015

Published: September 10, 2015

The kinetic data were used to calculate a rate constant of $4.05 \times 10^{-2} \text{ M}^{-1} \text{ s}^{-1}$ (entry 1 in Table 1) based on the initial

Table 1. Rate Constants for Epoxide Cleavage Inside $\{\text{Mo}_{132}\}$ Capsules at Room Temperature ($23 \pm 1 \text{ }^\circ\text{C}$)^{a,b}

Entry	Epoxide	Internal ligand	Number of internal ligands	Number of $\text{Mo}^{\text{V}}_2(\text{H}_2\text{O})_2$ active sites	Rate constant, k ($\text{M}^{-1}\text{s}^{-1} \times 10^{-2}$)
1			23	7	4.05
2			23	7	0.59
3			21	9	1.3
4			29	1	0.15
5			12	18	11.1
6		n.a.	n.a.	n.a.	0.0028 ^c

^aIn entries 1 and 2, 70 equiv of epoxide (250 mM) were added to NMR tubes containing the indicated capsules (3.61 mM), mixed by rapid agitation and immediately inserted into the NMR probe (for entries 3 and 4, 50 equiv of PO were added, and 175 equiv for entry 5). ^bSee Figure S2 for a ¹H NMR spectrum of the propanoate form of the capsule. ^cControl with acidified MoO_4^{2-} ; k was calculated per molar concentration of Na_2MoO_4 , adjusted to pH 4 by addition of methanesulfonic acid (see the SI for details). If calculated per molar concentration of octamolybdate (the dominant species at pH 4), the rate constant would be $0.022 \times 10^{-2} \text{ M}^{-1} \text{ s}^{-1}$.

rate (i.e., less than 10% conversion), and the concentrations of the substrate and capsule. For screening purposes, the same method was used to determine rate constants (also in Table 1) as functions of substrate size, internal-carboxylate-ligand size, and the numbers of ligand-blocked ($\text{Mo}^{\text{V}}_2\text{L}$) and activated (Mo^{V}_2) sites.

Entries 1–2 show that relative to the hydrolysis of PO, (entry 1), addition of a single methyl group decreases the rate constant by ca. 7-fold. Under identical control conditions (pH values, Na^+ , acetate ion, and molybdate concentration, but in the absence of the capsule; as used for the data in entry 6), the two substrates are hydrolyzed at effectively identical rates. Hence, steric factors appear to be at work. While the capsule's ca. 3 Å diameter Mo_3O_9 pores^{7,10} could certainly provide for size selectivity, this does not appear to be the case here. This is because early in the respective reactions, equal numbers of equivalents of encapsulated PO and *trans*-2,3-epoxybutane are observed by ¹H NMR. As such, the rate decrease is attributed to steric effects *inside* the capsule, arising from less effective approach of the larger *trans*-dimethyl substrate to Mo^{V}_2 active sites.

A type of noncompetitive inhibition was demonstrated by increasing the size and number of blocking ligands, L. In entry 3, L was changed from acetate to propanoate. In both cases, similar numbers of encapsulated substrate were observed inside the capsule.¹² The decrease in k is thus attributed to steric effects of the larger ligands on access to the Mo^{V}_2 active sites. When the number of propanoate ligands was increased from 21 to 29, however (entry 4), k decreased by a factor of 8.7, close to the 8-fold decrease in the number of Mo^{V}_2 sites.

Up-regulation was then demonstrated in a preliminary fashion by using dialysis against pure water to remove acetate ligands from the capsule. With only 12 acetate ligands bound within the capsule (entry 5), 18 Mo^{V}_2 sites are activated, resulting in the largest rate constant for PO hydrolysis. Notably,

upon increase in the number of Mo^{V}_2 sites by a factor of 2.6 (i.e., from 7 to 18; entries 1 and 5), the respective rate constants increase by a similar factor of 2.7, consistent with a linear response to the numbers of unblocked Mo^{V}_2 sites. This and the analogous response to numbers of propanoate ligands (above) provide definitive evidence that hydrolysis is catalyzed by reactions of encapsulated substrates.

The internally accessed Mo^{V}_2 sites are closely related to the hexaaqua complex, $[\text{Mo}^{\text{V}}_2\text{O}_4(\text{H}_2\text{O})_6]^{2+}$, which is only stable in 4 M aqueous HCl. (Derivatives stable at pH values relevant to the present work invariably contain polydentate ligands that leave no aqua-ligand-occupied coordination sites that, upon reversible loss of water, could serve as Lewis acids.) Importantly, the metal-oxide skeleton of the $\{\text{Mo}_{132}\}$ capsule stabilizes the Lewis-acidic $[\text{Mo}^{\text{V}}_2\text{O}_4(\text{H}_2\text{O})_2]^{2+}$ fragments at pH 4 to 5 in water.

At the same time, metal cations in water are generally poor Lewis acids because kinetically competent *aqua-ligand-free* (unsaturated) metal sites are present at very small concentrations.¹³ This suggests a second important role for the $\{\text{Mo}_{132}\}$ cage: its encapsulation of substrate guests increases the lifetimes during which they are held in close proximity to short-lived, *aqua-ligand-free* Mo^{V}_2 Lewis-acid sites.

The instability of $[\text{Mo}^{\text{V}}_2\text{O}_4(\text{H}_2\text{O})_6]^{2+}$ at pH 4–5, however, makes it difficult to compare the activities of the Mo^{V}_2 sites in $\{\text{Mo}_{132}\}$ with water-soluble models. Nevertheless, an indication of their considerably high reactivity was obtained using a control experiment in which PO was reacted with a pH 4 mixture of species, including the octamolybdate complex, $[\text{Mo}_8\text{O}_{26}]^{6-}$, obtained by acid condensation of Na_2MoO_4 (see entry 6 and caption).

To better understand the reactions in Table 1, a more detailed kinetic investigation was undertaken. This led to full documentation of Michaelis–Menten behavior,^{1e,4a,b,14} which, in turn, provided more information on the effect of the $\{\text{Mo}_{132}\}$ cage. Michaelis–Menten behavior was hinted at by the observation that, in the presence of $\{\text{Mo}_{132}\}$, PO was not only observed inside the capsule, but the ¹H NMR signals arising from the epoxide in bulk solution *outside* the capsule were unusually broad.

Figure 2 shows the ¹H NMR spectrum of pure PO at 25 °C (panel A) and in the presence of $\{\text{Mo}_{132}\}$ (panel B). To

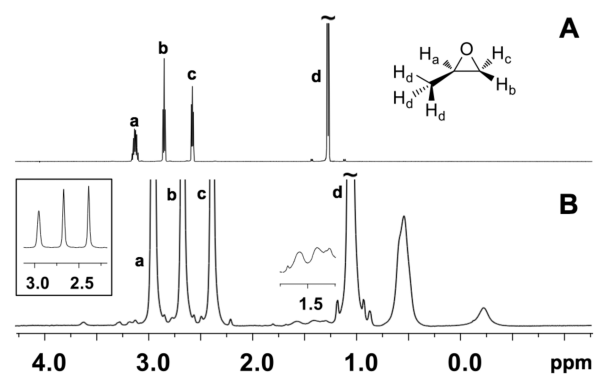
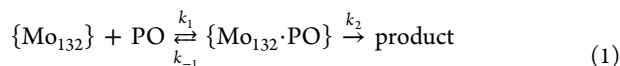


Figure 2. Proton-NMR spectra of propylene oxide (PO) in D_2O (A) and after adding 125 equiv to a 7.22 mM solution of $\{\text{Mo}_{132}\}$ (23 acetate ligands) at 5 °C (B). Broad signals of PO inside the capsule appear at 1.5 ppm (protons “a”, “b”, and “c”) and at -0.23 ppm (CH_3). The broad signal at ca. 0.6 ppm is due to the Me groups of the acetate ligands.

observe signals of encapsulated PO, the latter spectrum was acquired at 5 °C using a large capsule concentration of 7.22 mM and 125 equiv of the epoxide. Consistent with encapsulated PO, the ^1H NMR spectrum featured three broad⁹ signals at ca. 1.5 ppm (inset), assigned to protons “a”, “b”, and “c”, and one at ca. –0.23, assigned to the CH_3 protons, “d”. (Related COSY and DOSY spectra are provided in Figure S3.) Even in the absence of exchange, broadening is typical in ^1H NMR spectra of encapsulated guests,⁹ and the broad signals consistently appear at chemical-shift values 1.2–1.4 ppm upfield of those from corresponding protons of the same molecules in bulk solution outside the capsule.^{15,16} As such, the broad signal at –0.23 ppm (inset) is upfield by ca. 1.3 ppm of the CH_3 signal, labeled “d”, of PO in bulk solution. The signals at 1.5 ppm (inset) are ca. 1.2 ppm upfield of the average position of the three signals (“a”, “b”, and “c”), centered at ca. 2.7 ppm. Finally, the signals at 1.5 and –0.23 ppm are too far upfield to arise from encapsulated 1,2-diol (cf. Figure 1C).

As noted above, the signals due to PO in bulk solution (labeled “a”, “b”, and “c”, and “on scale” in the inset at the far left in panel B) are broadened by the presence of $\{\text{Mo}_{132}\}$, both at 5 °C (shown here) and at 25 °C (Figures 1B and S4), suggesting a dynamic process involving reversible encapsulation of PO.

The presence of PO inside the capsule, in combination with the broadening evident in panel B, pointed to a pre-equilibrium involving rapid entry/exit of the intact substrate (k_1/k_{-1} in eq 1; the number of encapsulated PO molecules is not indicated), followed by rate-limiting hydrolysis at MoV_2 active sites inside the capsule (k_2).



This situation is formally identical to the reversible substrate binding at saturated enzyme active sites described by Michaelis–Menten kinetics. To investigate this, initial reaction rates (V , in units of M sec^{-1} of hydrolysis products) were obtained as a function of PO concentration. When plotted, the data revealed a classical Michaelis–Menten rate profile (Figure 3A). Strict compliance with Michaelis–Menten kinetics was

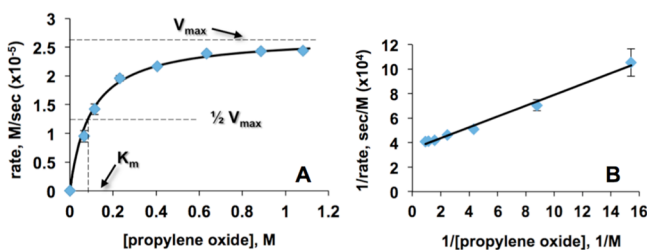


Figure 3. Michaelis–Menten (A) and Lineweaver–Burk plots (B) for the capsule with 23 acetate ligands. (A) V_{max} is the rate at “infinite” $[\text{PO}]$, and K_m is the Michaelis–Menten constant ($[\text{PO}]$ at $1/2V_{\text{max}}$). (B) A plot of $1/V$ as a function of $1/[\text{S}]$ (eq 2). The slope is K_m/V_{max} and the y -intercept is $1/V_{\text{max}}$. Experimental uncertainties in $1/V$ are indicated by vertical lines with horizontal bars.

confirmed by plotting the rate data (values of V) according to eq 2 in which $[\text{S}] = [\text{PO}]$. This gave the Lineweaver–Burk plot in Figure 3B, with an excellent fit of $R^2 = 0.99$.

$$\frac{1}{V} = \frac{K_m + [\text{S}]}{K_{\text{max}}[\text{S}]} = \frac{K_m}{V_{\text{max}}} \cdot \frac{1}{[\text{S}]} + \frac{1}{V_{\text{max}}} \quad (2)$$

The slope and y -intercept (see caption to Figure 3) gave $K_m = 9.62 \times 10^{-2} \text{ M}$ and $V_{\text{max}} = 2.69 \times 10^{-5} \text{ M s}^{-1}$. The latter value was used to calculate a turnover rate, $k_{\text{cat}} (V_{\text{max}}/[\{\text{Mo}_{132}\}])$, of $7.43 \times 10^{-3} \text{ s}^{-1}$.

To determine the rate enhancement, $k_{\text{cat}}/k_{\text{uncat}}$, the uncatalyzed rate of PO cleavage was determined in D_2O at $296 \pm 1 \text{ K}$. The pD of the solution was first adjusted to 4.3 (by adding a few microliters of dilute methanesulfonic acid) to match the slight acidity obtained upon dissolution of the $\{\text{Mo}_{132}\}$ capsule. The observed k_{uncat} value ($4.65 \times 10^{-7} \text{ s}^{-1}$) gave a rate acceleration of $k_{\text{cat}}/k_{\text{uncat}} = 16,000$. Upon “up-regulation” by dialysis against pure water¹⁷ 11 additional blocking ligands were removed from the capsule, giving 18 activated MoV_2 sites. In response, k_{cat} increased to $8.50 \times 10^{-2} \text{ s}^{-1}$, and the rate enhancement increased from 16,000 to $182,800 \pm 500$.¹⁸

These values, in combination with data from Table 1, make it possible to differentiate between the effect of increasing the number of MoV_2 active sites, and a “cage effect” related to an increase in the effective molarity of the reaction.¹⁹ Upon increase from seven to 18 active MoV_2 sites (Table 1, entries 1 and 5), the rate constant increased by a factor of 18/7 or 2.6. Those data were obtained using relatively small concentrations of PO, far from saturation (V_{max}) of the 12-acetate-ligand capsule. Under those conditions, the reaction is first-order in the number of MoV_2 sites. As such, the 2.6-fold increase in numbers of active sites should increase the rate acceleration at V_{max} ($k_{\text{cat}}/k_{\text{uncat}}$) by a factor of 2.6, from 16,000 to 43,200, far short of the observed value of 182,800.

Notably, however, the decrease from 23 to 12 acetate ligands (to give 18 active MoV_2 sites) considerably increases the space available for substrate molecules inside the capsule. As a result, the steady-state number of PO “guests” inside the capsule at saturation nearly doubles from 5 ± 0.5 (23 acetate ligands) to 9 ± 0.5 (12 acetate ligands). Hence, not only are more MoV_2 active sites present, but the concentration of encapsulated substrate increases as well. This increases the effective molarity of the reaction, thereby amplifying the rate acceleration per MoV_2 active site. This cage effect increases the rate acceleration from 43,200 (based on the larger number of MoV_2 sites) to an enzyme-like^{4c} value of 182,000.

The present findings demonstrate how the structural framework of a porous capsule can stabilize reactive metal fragments in water, and through encapsulation, bring numerous guest substrates in close proximity to multiple active sites. We further show how the removal of endohedrally bound blocking ligands increases turnover rates by providing a larger number of reactive (ligand-free) metal sites, whose activity, in turn, is simultaneously amplified by a larger steady-state concentration of encapsulated substrates, more of which now occupy the larger interior space of the ligand-depleted cage.

■ ASSOCIATED CONTENT

Supporting Information

The Supporting Information is available free of charge on the ACS Publications website at DOI: 10.1021/jacs.5b06211.

Materials and methods, and spectra (PDF)

■ AUTHOR INFORMATION

Corresponding Author

*iraw@bgu.ac.il

Notes

The authors declare no competing financial interest.

ACKNOWLEDGMENTS

Support from the ISF (190/13 to I.A.W.), the Kreitman Foundation (to S.K.), the Deutsche Forschungsgemeinschaft (to A.M.) and the ERC (Advanced Grant to A.M.). The authors thank Drs. Sabine Akabayov and Amira Rudi for their input on multi-dimensional NMR spectra.

REFERENCES

- (1) For cages and containers: (a) Cook, T. R.; Stang, P. J. *Chem. Rev.* **2015**, *115*, 7001–7045. (b) Brown, C. J.; Toste, F. D.; Bergman, R. G.; Raymond, K. N. *Chem. Rev.* **2015**, *115*, 3012–3035. (c) Leenders, S. H. A. M.; Gramage-Doria, R.; de Bruin, B.; Reek, J. N. H. *Chem. Soc. Rev.* **2015**, *44*, 433–448. (d) Ballester, P.; Fujita, M.; Rebek, J., Jr. *Chem. Soc. Rev.* **2015**, *44*, 392–393. (e) Amouri, H.; Desmarets, C.; Moussa, J. *Chem. Rev.* **2012**, *112*, 2015–2041. (f) Ajami, D.; Rebek, J. *Acc. Chem. Res.* **2013**, *46*, 990–999. (g) Wiester, M. J.; Ulmann, P. A.; Mirkin, C. A. *Angew. Chem., Int. Ed.* **2011**, *50*, 114–137.
- (2) (a) Garcia-Simon, C.; Gramage-Doria, R.; Raoufoghaddam, S.; Parella, T.; Costas, M.; Ribas, X.; Reek, J. N. H. *J. Am. Chem. Soc.* **2015**, *137*, 2680–2687. (b) Zhao, C.; Toste, F. D.; Raymond, K. N.; Bergman, R. G. *J. Am. Chem. Soc.* **2014**, *136*, 14409–14412.
- (3) (a) Lifschitz, A. M.; Young, R. M.; Mendez-Arroyo, J.; Stern, C. L.; McGuirk, C. M.; Wasielewski, M. R.; Mirkin, C. A. *Nat. Commun.* **2015**, *6*, 6541. (b) Preston, D.; Fox-Charles, A.; Lo, W. K. C.; Crowley, J. D. *Chem. Commun.* **2015**, *51*, 9042–9045. (c) Kremer, C.; Luetzen, A. *Chem. - Eur. J.* **2013**, *19*, 6162–6196.
- (4) (a) Hastings, C. J.; Pluth, M. D.; Bergman, R. G.; Raymond, K. N. *J. Am. Chem. Soc.* **2010**, *132*, 6938–6940. (b) Marinescu, L. G.; Bols, M. *Angew. Chem., Int. Ed.* **2006**, *45*, 4590–4593. (c) Trainor, G. L.; Breslow, R. *J. Am. Chem. Soc.* **1981**, *103*, 154–158.
- (5) Horiuchi, S.; Murase, T.; Fujita, M. *Angew. Chem., Int. Ed.* **2012**, *51*, 12029–12031.
- (6) This is emphasized in the “Future Directions” section of a 2011 review by Mirkin (ref 1g), and in the “Conclusions and Outlook” section of a 2015 review by Brown, Troste, Bergman, and Raymond (ref 1b). For examples, see: (a) Kohyama, Y.; Murase, T.; Fujita, M. *J. Am. Chem. Soc.* **2014**, *136*, 2966–2969. (b) Metherell, A. J.; Ward, M. D. *Chem. Commun.* **2014**, *50*, 6330–6332. (c) Lee, S. J.; Cho, S.-H.; Mulfort, K. L.; Tiede, D. M.; Hupp, J. T.; Nguyen, S. T. *J. Am. Chem. Soc.* **2008**, *130*, 16828–16829. (d) Brisig, B.; Sanders, J. K. M.; Otto, S. *Angew. Chem., Int. Ed.* **2003**, *42*, 1270–1273. (e) Nakash, M.; Clyde-Watson, Z.; Feeder, N.; Davies, J. E.; Teat, S. J.; Sanders, J. K. M. *J. Am. Chem. Soc.* **2000**, *122*, 5286–5293. (f) Mackay, L. G.; Wylie, R. S.; Sanders, J. K. M. *J. Am. Chem. Soc.* **1994**, *116*, 3141–3142. (g) Walter, C. J.; Anderson, H. L.; Sanders, J. K. M. *J. Chem. Soc., Chem. Commun.* **1993**, 458–460.
- (7) (a) Müller, A.; Gouzerh, P. *Chem. - Eur. J.* **2014**, *20*, 4862–4873. (b) Müller, A.; Gouzerh, P. *Chem. Soc. Rev.* **2012**, *41*, 7431–7463.
- (8) (a) Johnson, A. M.; Wiley, C. A.; Young, M. C.; Zhang, X.; Lyon, Y.; Julian, R. R.; Hooley, R. J. *Angew. Chem., Int. Ed.* **2015**, *54*, 5641–5645. (b) Jayamurugan, G.; Roberts, D. A.; Ronson, T. K.; Nitschke, J. R. *Angew. Chem., Int. Ed.* **2015**, *54*, 7539–7543. (c) Gütz, C.; Hovorka, R.; Klein, C.; Jiang, Q.-Q.; Bannwarth, C.; Engeser, M.; Schmuck, C.; Assenmacher, W.; Mader, W.; Topić, F.; Rissanen, K.; Grimme, S.; Lützen, A. *Angew. Chem., Int. Ed.* **2014**, *53*, 1693–1698. (d) Bruns, C. J.; Fujita, D.; Hoshino, M.; Sato, S.; Stoddart, J. F.; Fujita, M. *J. Am. Chem. Soc.* **2014**, *136*, 12027–12034. (e) Zhao, L.; Ghosh, K.; Zheng, Y.-R.; Stang, P. J. *J. Org. Chem.* **2009**, *74*, 8516–8521. (f) Sato, S.; Iida, J.; Suzuki, K.; Kawano, M.; Ozeki, T.; Fujita, M. *Science* **2006**, *313*, 1273–1276.
- (9) (a) Grego, A.; Mueller, A.; Weinstock, I. A. *Angew. Chem., Int. Ed.* **2013**, *52*, 8358–8362. (b) Petina, O.; Rehder, D.; Haupt, E. T. K.; Grego, A.; Weinstock, I. A.; Merca, A.; Boegge, H.; Szakacs, J.; Mueller, A. *Angew. Chem., Int. Ed.* **2011**, *50*, 410–414.
- (10) Ziv, A.; Grego, A.; Kopilevich, S.; Zeiri, L.; Miro, P.; Bo, C.; Muller, A.; Weinstock, I. A. *J. Am. Chem. Soc.* **2009**, *131*, 6380–6382.
- (11) Kopilevich, S.; Gil, A.; Garcia-Ratés, M.; Bonet-Ávalos, J.; Bo, C.; Müller, A.; Weinstock, I. A. *J. Am. Chem. Soc.* **2012**, *134*, 13082–13088.
- (12) ¹H NMR data showed 4.5 ± 0.5 equiv of PO in the capsules with 23 acetate ligands and 21 propanoate ligands (entries 1 and 3), and 5 ± 1 equiv in the capsule with 29 propanoate ligands (entry 4). At small [PO], reaction by the 12-acetate capsule is too rapid for reliable quantification, but the number of equiv of encapsulated PO is < 7.
- (13) Kobayashi, S.; Manabe, K. *Acc. Chem. Res.* **2002**, *35*, 209–217.
- (14) (a) Dydio, P.; Detz, R. J.; Reek, J. N. H. *J. Am. Chem. Soc.* **2013**, *135*, 10817–10828. (b) Pluth, M. D.; Bergman, R. G.; Raymond, K. N. *Acc. Chem. Res.* **2009**, *42*, 1650–1659. (c) Ortega-Caballero, F.; Rousseau, C.; Christensen, B.; Petersen, T. E.; Bols, M. *J. Am. Chem. Soc.* **2005**, *127*, 3238–3239.
- (15) Schäffer, C.; Todea, A. M.; Bögge, H.; Petina, O. A.; Rehder, D.; Haupt, E. T. K.; Müller, A. *Chem. - Eur. J.* **2011**, *17*, 9634–9639.
- (16) Kozik, M.; Casan-Pastor, N.; Hammer, C. F.; Baker, L. C. W. *J. Am. Chem. Soc.* **1988**, *110*, 7697–7701.
- (17) This was done by dialysis against water (see the Supporting Information). Notably, “flow” methods could be used with porous membranes to continuously modify capsule reactivity.
- (18) To our knowledge, this is the largest rate acceleration reported to date for a cage or container in pure water at room temperature. See ref 1b for a discussion of reported rate accelerations.
- (19) Cacciapaglia, R.; Di Stefano, S.; Mandolini, L. *Acc. Chem. Res.* **2004**, *37*, 113–122.